Journal of Controlled Release 282 (2018) 131–139

Contents lists available at ScienceDirect

Journal of Controlled Release

journal homepage: www.elsevier.com/locate/jconrel

Dual TLR agonist nanodiscs as a strong adjuvant system for vaccines and immunotherapy

Rui Kuai[a,b], Xiaoqi Sun[a,b], Wenmin Yuan[a,b], Lukasz J. Ochyl[a,b], Yao Xu[a,b], Alireza Hassani Najafabadi[a,b], Lindsay Scheetz[a,b], Min-Zhi Yu[a,b], Ishina Balwani[a,b], Anna Schwendeman[a,b,*], James J. Moon[a,b,c,*]

[a] Department of Pharmaceutical Sciences, University of Michigan, Ann Arbor, MI 48109, USA
[b] Biointerfaces Institute, University of Michigan, Ann Arbor, MI 48109, USA
[c] Department of Biomedical Engineering, University of Michigan, Ann Arbor, MI 48109, USA

ARTICLE INFO

Keywords:
Vaccine
Nanoparticle
Adjuvant
Cancer
Immunotherapy

ABSTRACT

Recent studies have shown that certain combinations of Toll-like receptor (TLR) agonists can induce synergistic immune activation. However, it remains challenging to achieve such robust responses in vivo in a manner that is effective, facile, and amenable for clinical translation. Here, we show that MPLA, a TLR4 agonist, and CpG, a TLR9 agonist, can be efficiently co-loaded into synthetic high-density lipoprotein nanodiscs, forming a potent adjuvant system (ND-MPLA/CpG) that can be readily combined with a variety of subunit antigens, including proteins and peptides. ND-MPLA/CpG significantly enhanced activation of dendritic cells, compared with free dual adjuvants or nanodiscs delivering a single TLR agonist. Importantly, mice immunized with physical mixtures of protein antigens ND-MPLA/CpG generated strong humoral responses, including induction of IgG responses against protein convertase subtilisin/kexin 9 (PCSK9), leading to 17–30% reduction of the total plasma cholesterol levels. Moreover, ND-MPLA/CpG exerted strong anti-tumor efficacy in multiple murine tumor models. Compared with free adjuvants, ND-MPLA/CpG admixed with ovalbumin markedly improved antigen-specific CD8+ T cell responses by 8-fold and promoted regression of B16F10-OVA melanoma ($P < 0.0001$). Furthermore, ND-MPLA/CpG admixed with E7 peptide antigen elicited ~20% E7-specific CD8+ T cell responses and achieved complete regression of established TC-1 tumors in all treated animals. Taken together, our work highlights the simplicity, versatility, and potency of dual TLR agonist nanodiscs for applications in vaccines and cancer immunotherapy.

1. Introduction

Vaccination is a powerful medical intervention that is proven to be effective in the settings of infectious diseases, cancer, and many pathologies [1–3]. Compared with live attenuated or killed vaccines, vaccines based on subunit antigens, such as recombinant proteins or peptide antigens, are more attractive due to their safety and ease of manufacturing and quality control [4–7]. However, because of their low immunogenicity, subunit antigens need to be administered with immune-stimulating adjuvants to promote immune responses [8]. Among various adjuvant molecules, Toll-like receptor (TLR) agonists have been studied extensively [9,10]. TLR agonists can activate dendritic cells to upregulate costimulatory ligands and secrete pro-inflammatory cytokines, thereby providing critical signals to the adaptive immune system for induction of cellular and humoral immune responses [11].

Notably, recent studies have indicated synergy between various combinations of TLR agonists [12,13]. Specifically, monophosphoryl lipid A (MPLA, a TLR4 agonist) and CpG-rich oligonucleotide (CpG, a TLR9 agonist) activate dendritic cells (DCs) via two distinct pathways. MPLA triggers the interferon regulatory factor 3 (IRF3) pathway via Toll/IL-1R domain-containing adaptor inducing IFN-β (TRIF) and is currently used in the clinic [10,14,15]. CpG activates nuclear factor kappa B (NF-KB) via myeloid differentiation primary response gene 88 (MyD88) [16–18], and a hepatitis B vaccine (HEPLISAV-B™, Dynavax Technologies Corporation, Berkeley, CA) containing CpG oligonucleotide-1018 as an adjuvant was approved by the US Food and Drug Administration (FDA) for clinical use on November 9, 2017 [19]. Importantly, potent synergy between TLR4 and TLR9 agonists in activation of antigen-presenting cells has been documented in vitro

* Corresponding authors at: Department of Pharmaceutical Sciences, University of Michigan, Ann Arbor, MI 48109, USA.
E-mail addresses: annaschw@umich.edu (A. Schwendeman), moonjj@umich.edu (J.J. Moon).

https://doi.org/10.1016/j.jconrel.2018.04.041
Received 15 January 2018; Received in revised form 23 April 2018; Accepted 23 April 2018
Available online 25 April 2018
0168-3659/ © 2018 Published by Elsevier B.V.

[12,13], and their in vivo efficacy to generate adaptive immune responses have been recently reported using adjuvant delivery systems [20–23]. Despite these advances, there is still a need for a general methodology that can achieve potent immune activation with combinations of TLR agonists, especially in a manner that is effective, facile, and amenable for clinical translation.

Here, we propose a simple strategy for co-delivering multiple TLR agonists in vivo that can be readily formulated with a variety of subunit antigens. Previously, synthetic high-density lipoprotein (sHDL), either made from recombinant apolipoproteins or obtained from endogenous plasma has been examined as delivery vehicles for various cargo molecules [24–27]. In our own prior work, we have reported the development of sHDL nanodiscs (ND), composed of biocompatible phospholipids and apolipoprotein A1 (ApoA1)-mimetic peptide [28]. We have demonstrated their versatility to deliver a wide range of therapeutics, including chemotherapeutics, imaging agents, and nucleic acids [28–32]. Additionally, we have recently shown that ND loaded with peptide antigens and a TLR9 agonist efficiently drained to local draining lymph nodes and induced strong antigen-specific T cell responses against cancer cells [33]. Here, we show that ND serves as an effective delivery platform for dual TLR agonists and demonstrate their adaptability and potency with a range of subunit antigens, including protein and peptide antigens.

In this current study, we report that sHDL ND allowed for efficient incorporation (> 80% efficiency) of MPLA. Additionally, as sHDL ND is a good acceptor for cholesterol [28], we have employed cholesterol-modified CpG for loading into sHDL ND and achieved > 95% incorporation efficiency for CpG. The resulting ND co-loaded with the dual adjuvants (ND-MPLA/CpG) was more effective at activation and maturation of DCs, compared with free dual adjuvants or even ND containing either MPLA or CpG. Immunizations with ND-MPLA/CpG physically mixed with protein antigens generated strong humoral immune responses in vivo, including induction of antibody responses against protein convertase subtilisin/kexin 9 (PCSK9), leading to 17–30% reduction of the total plasma cholesterol levels in mice. Importantly, ND-MPLA/CpG also served as a potent adjuvant system for elicitation of cellular immune responses in vivo. Compared with free adjuvants, ND-MPLA/CpG admixed with a model antigen protein, ovalbumin (OVA), significantly improved antigen-specific CD8+ T cell responses in B16F10-OVA tumor-bearing mice, inducing regression of established melanoma tumors. Finally, we have also confirmed these results using the TC-1 tumor cell line expressing the E7 oncogene from human papillomavirus (HPV) type 16. Immunizations with ND-MPLA/CpG admixed with E7 antigen peptide elicited ~20% E7-specific antigen-specific CD8+ T cells and exerted potent anti-tumor efficacy against established TC-1 tumors. Overall, our results demonstrate that ND-MPLA/CpG is a promising adjuvant system for vaccination and immunotherapy.

2. Materials & methods

2.1. Reagents

1,2-Dimyristoyl-sn-glycero-3-phosphocholine (DMPC) was purchased from Nippon Oils and Fats (Osaka, Japan). ApoA1 mimetic peptide 22A (PVLDLFRELLNELLEALKQKLK) was synthesized by GenScript Corp (Piscataway, NJ). MPLA was purchased from Avanti Polar Lipids (Alabaster, AL). 1,1′-Dioctadecyl-3,3,3′,3′-Tetramethylindodicarbocyanine, 4-chlorobenzenesulfonate salt (DiD) was purchased from Invitrogen. CpG1826 modified with cholesterol at the 3′ end (labeled as CpG throughout this manuscript) was synthesized by Integrated DNA Technologies (Coralville, IA). Ovalbumin (OVA) was purchased from Worthington (Lakewood, NJ). Recombinant human protein convertase subtilisin/kexin 9 (hPCSK9) was purchased from BioLegend (San Diego, CA). Recombinant mouse PCSK9 (mPCSK9) was purchased from Abcam (Cambridge, MA). E7 (GQAEPDRAHYNIVTFCCKCD) peptide was synthesized by Anaspec (Fremont, CA). Fetal bovine serum (FBS), penicillin-streptomycin, β-mercaptoethanol and ACK lysis buffer were purchased from Life Technologies (Grand Island, NY). Granulocyte-macrophage colony stimulating factor (GM-CSF) was from GenScript Corp. (Piscataway, NJ). Anti-mouse CD16/32, CD80, CD86 were from eBioscience (San Diego, CA). Anti-mouse CD8α-APC was from BD Bioscience (San Jose, CA). Tetramer H-2Kb-SIINFEKL-PE was purchased from Beckman Coulter (Brea, CA). Tetramer H-2Db-RAHYNIVTF-BV421 was kindly provided by the NIH Tetramer Core Facility (Atlanta, GA).

2.2. Preparation of ND-MPLA/CpG

sHDL nanodiscs (ND) were prepared by using the lyophilization method, as we reported previously [29,31,32]. To load MPLA into ND, MPLA was co-dissolved with DMPC and 22A at the weight ratio of 0.01:2:1 in acetic acid, followed by lyophilization and hydration with PBS to form ND-MPLA. To load CpG in ND-MPLA, CpG1826 modified with cholesterol at the 3′ end (i.e. CpG) was incubated with pre-formed ND-MPLA for 30 min at room temperature. In some experiments, 0.3% mol of DiD was mixed with lipids to prepare DiD-labeled nanodiscs.

2.3. Characterization of ND-MPLA/CpG

The loading efficiency of MPLA in ND-MPLA was measured by HPLC equipped with an evaporative light scattering detector (ELSD) as described before [34]. The loading efficiency of CpG was measured by gel permeation chromatography (GPC), as we reported previously [33]. Briefly, ND samples were injected in a Shimadzu HPLC system equipped with a TSKgel G2000SWxl column (7.8 mm ID × 30 cm, Tosoh Bioscience LLC), and the amount of CpG was quantified with the detection wavelength set at 280 nm. The particle size of ND-MPLA/CpG was measured by dynamic light scattering (DLS) on a Malvern Zetasizer (Westborough, MA). The ND morphology was assessed by transmission electron microscopy (TEM). Properly diluted ND sample solution was deposited on a carbon film-coated 400 mesh copper grid (Electron Microscopy Sciences) and dried for 1 min. The ND samples were then negatively stained with 1% (w/v) uranyl formate, and the grid was dried before TEM observation. All specimens were imaged on a 100 kV Morgagni TEM equipped with a Gatan Orius CCD.

2.4. Cell culture

Bone marrow-derived dendritic cells (BMDCs) were prepared as described previously [35]. Briefly, femur and tibia were harvested aseptically from C57BL/6 mice, and the bone marrow was flushed into a petri dish using a 5 mL syringe (26 G needle) loaded with BMDC culture media (RPMI 1640 supplemented with 10% FBS, 100 U/mL penicillin, 100 μg/mL streptomycin, 50 μM β-mercaptoethanol, and 20 ng/mL GM-CSF). Cells were collected by passing the cell suspension through a cell strainer (mesh size = 40 μm), followed by centrifugation. Cells were seeded into non-tissue culture treated petri-dish at a density of 2×10^5 cells/mL, cultured at 37 °C with 5% CO_2. Culture media were refreshed on days 3, 6, 8, and 10, and BMDCs were used for the following assays on days 8–12. B16F10-OVA cells were kindly provided by Dr. Darrell Irvine at Massachusetts Institute of Technology MIT (Cambridge, MA). TC-1 cells were kindly provided by Dr. T. C. Wu at Johns Hopkins University (Baltimore, MD). The TC-1 tumor model was generated by transformation of primary lung epithelial cells from C57BL/6 mice with active Ras together with HPV-16 E6 and E7 oncogenes [36]. Both cell lines were maintained in RPMI1640 medium supplemented with 10% FBS, 100 U/mL penicillin and 100 μg/mL streptomycin. HEK cells transfected with TLR2, TLR4, or TLR9 (InvivoGen, San Diego, CA) were incubated with nanodiscs containing 0.5 μg/mL CpG and/or 0.05 μg/mL MPLA for 24 h, and activation of TLR signaling pathways was detected by following the manufacturer's instructions.

2.5. BMDC activation

Immature BMDCs were plated at 1×10^6 cells/well in 12-well plates. After 24 h, BMDCs were washed once with PBS and incubated with formulations containing 0.5 μg/mL CpG and/or 0.05 μg/mL MPLA for 24 h at 37 °C with 5% CO_2. After 24 h of incubation, the levels of IL-12p70 in the supernatant were measured by the ELISA kit (R&D systems) following the manufacturer's instructions. Uptake of NDs by BMDCs was measured after incubating BMDCs with nanodiscs containing 0.3% mol of DiD. To measure the levels of co-stimulatory markers, BMDCs incubated with ND samples were harvested, washed with FACS buffer (1% BSA in PBS), incubated with anti-CD16/32 at room temperature for at least 10 min, and then stained with fluorophore-labeled antibodies against CD80, and CD86 at room temperature for 30 min. Finally, the cells were washed twice with FACS buffer, resuspended in 2 μg/mL DAPI solution, and analyzed by flow cytometry (Cyan 5, Beckman Coulter, USA).

2.6. In vivo immunization study

Animals were cared for following federal, state, and local guidelines. All work performed on animals was in accordance with and approved by University Committee on Use and Care of Animals (UCUCA) at the University of Michigan, Ann Arbor. For the OVA vaccination study, female C57BL/6 mice of age 6–8 weeks (Envigo) were vaccinated 3 times in a 2-week interval by subcutaneous injection in the tail base, each with 10 μg OVA protein dose admixed with indicated adjuvants. For the PCSK9 vaccination study, female Balb/c mice of age 6–8 weeks (Envigo) were vaccinated 3 times in an 1-week interval by subcutaneous injection in the tail base with 0.5–4 μg/dose (0.5 μg/dose for primary vaccination and 4 μg/dose for the two booster vaccinations) of recombinant human PCSK9 (hPCSK9) admixed with indicated adjuvants containing 10 μg/dose CpG and 1 μg/dose MPLA. Serum cholesterol levels at indicated time points were measured using the commercially available Wako Cholesterol E kit (Wako Chemicals, Richmond, VA).

2.7. Therapeutic study in tumor-bearing mice

For the therapeutic vaccination studies in B16F10-OVA tumor-bearing animals, C57BL/6 mice were inoculated subcutaneously with 2×10^5 B16F10-OVA cells on day 0 and vaccinated on days 7, and 13 with indicated formulations containing 10 μg/dose of OVA protein, 10 μg/dose of CpG and/or 1 μg/dose of MPLA. For the therapeutic tumor vaccination studies in TC-1 tumor-bearing animals, C57BL/6 mice were inoculated subcutaneously with 2×10^5 TC-1 cells on day 0 and vaccinated by subcutaneous injection in the tail base on days 8 and 14 with the indicated formulations containing 10 μg/dose of E7 peptide, 10 μg/dose of CpG, and 1 μg/dose of MPLA. Tumor growth was monitored every other day, and the tumor volume was calculated using the following equation [37]: tumor volume = length × width^2 × 0.52. Animals were euthanized when the tumor masses reached 1.5 cm in diameter or when animals became moribund with severe weight loss or ulceration.

2.8. Cellular responses induced by ND-MPLA/CpG

Immunized mice were analyzed for the percentages of antigen-specific CD8α + T cells among peripheral blood mononuclear cells (PBMCs) using the tetramer staining assay, as we described previously [38]. In brief, 100 μL of blood was drawn from each mouse on indicated time points by submandibular bleeding, and red blood cells were lysed with ACK lysis buffer. PBMCs were then washed with FACS buffer and blocked by anti-CD16/32 antibody and incubated with peptide-MHC tetramer (e.g. H-2K^b-restricted SIINFEKL or H-2D^b-restricted RAHYNIVTF) for 30 min at room temperature. Samples were then incubated with anti-CD8α-APC for 20 min on ice. Cells were washed twice with FACS buffer and resuspended in 2 μg/mL DAPI or 0.5 μg/mL 7AAD solution for analysis by flow cytometry (Cyan 5, Beckman Coulter, USA).

2.9. Humoral responses

ELISA plates were coated with OVA in PBS (1 μg/mL) or mPCSK9 in PBS (0.2 μg/mL) with 100 μL/well and incubated overnight at 4 °C. Plates were blocked with 1% BSA in PBS for 2 h, and 100 μL of serum in 4-fold serial dilutions was added to 96-well and incubated for 1 h at room temperature. After washing, wells were incubated with rabbit anti-mouse IgG-HRP (1:10000 dilution) for 1 h at room temperature, followed by addition of the HRP substrate, TMB. The enzymatic reaction was stopped by adding 2 N H_2SO_4, and the absorbance at 450 nm (OD450) was measured using a microplate reader. The highest dilution with twice the absorbance of background was considered as the end-point dilution titer [39].

2.10. Statistical analysis

All animal studies were performed after randomization. Data were analyzed by one- or two-way analysis of variance (ANOVA), followed by Tukey's multiple comparisons post-test, or log-rank (Mantel-Cox) test with Prism 6.0 (GraphPad Software). P values < 0.05 were considered statistically significant. All values are reported as means ± SEM with the indicated sample size. No samples were excluded from analysis.

3. Results and discussion

3.1. Preparation and characterization of adjuvant-loaded nanodiscs

Nanodiscs (ND) containing MPLA and/or CpG were prepared by the lyophilization method (Fig. 1a) [29,31,32]. Briefly, MPLA was added together with DMPC and 22A in acetic acid, followed by lyophilization and hydration in PBS to form ND containing MPLA (ND-MPLA). As measured by HPLC equipped with ELSD, MPLA was efficiently loaded onto ND with over 80% incorporation efficiency, likely due to the lipid-like properties of MPLA [40]. As visualized by TEM, ND samples were homogeneous with the average diameter of 10 nm (Fig. 1b). To co-load MPLA and CpG into ND samples, pre-formed ND-MPLA was incubated with cholesterol modified CpG for 30 min at room temperature (Fig. 1a). The incorporation efficiency of CpG as determined by GPC was over 95%, as long as the amount of CpG added was < 200 μg/mL per 2 mg/mL (lipid amount) of ND (Fig. 1c). When > 400 μg/mL of CpG was added, a significant amount of CpG remained unincorporated (Fig. 1c). Based on this, we chose to use no > 200 μg/mL of CpG to prepare CpG-loaded ND samples. We also examined the hydrodynamic size of ND-MPLA/CpG with DLS immediately after synthesis versus after an extended storage. ND-MPLA/CpG samples that were lyophilized, stored for 2 months at −20 °C, and reconstituted in endotoxin-free water exhibited an essentially equivalent hydrodynamic size of 10.1 ± 0.8 nm as freshly prepared ND-MPLA/CpG samples (Fig. 1d), indicating their suitability for long-term storage. Overall, these results indicate that adjuvant-loaded nanodiscs are homogenous and ultra-small in size, which may contribute to efficient lymph node draining as we have shown previously [33]. In addition, these dual adjuvant nanodiscs can be readily stored in a lyophilized form for an extended period of time without affecting their size and homogeneity, which may facilitate the transport, storage, and clinical use of adjuvant-loaded nanodiscs.

3.2. Potent DC activation by adjuvant-loaded nanodiscs

One of the major effects of adjuvants is to induce costimulatory

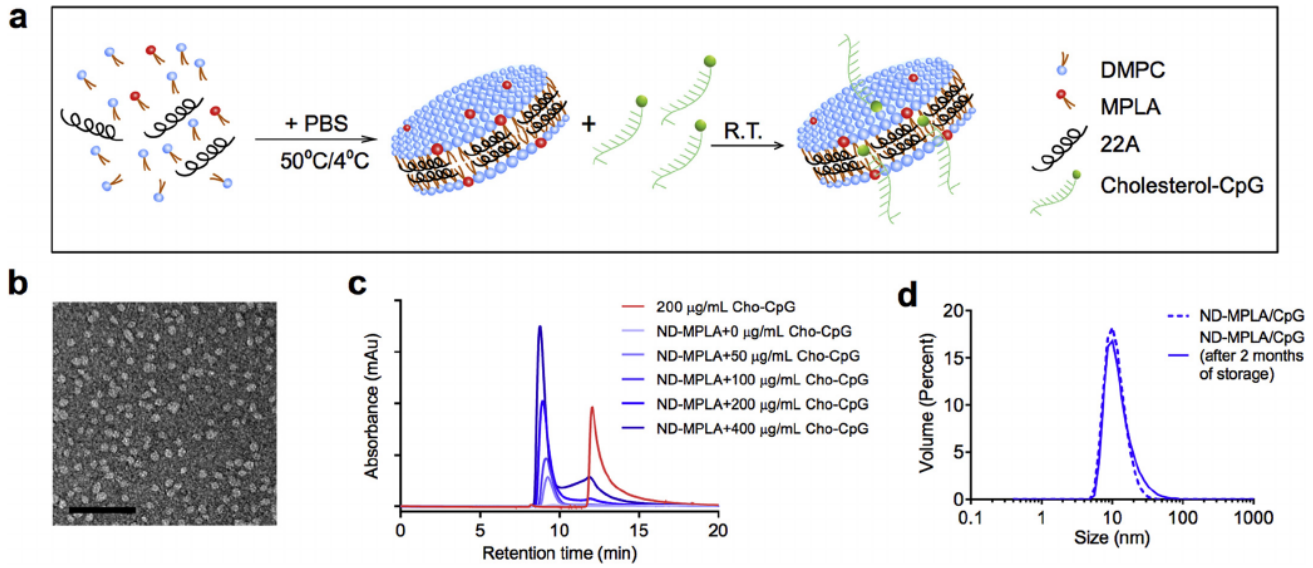

Fig. 1. Preparation and characterization of dual adjuvant nanodiscs. (a) Schematic for preparation of dual adjuvant nanodiscs (ND-MPLA/CpG). (b) TEM of nanodiscs, scale bar = 100 nm. (c) When ND-MPLA was incubated with different concentrations (0, 50, 100, 200, and 400 μg/mL) of Cho-CpG for 30 min at room temperature, Cho-CpG at concentrations lower than 200 μg/mL were efficiently loaded onto ND with over 95% efficiency. (d) The sizes of freshly prepared ND-MPLA/CpG versus freeze-dried ND-MPLA/CpG reconstituted with endotoxin-free water after 2 months of storage at 20 °C.

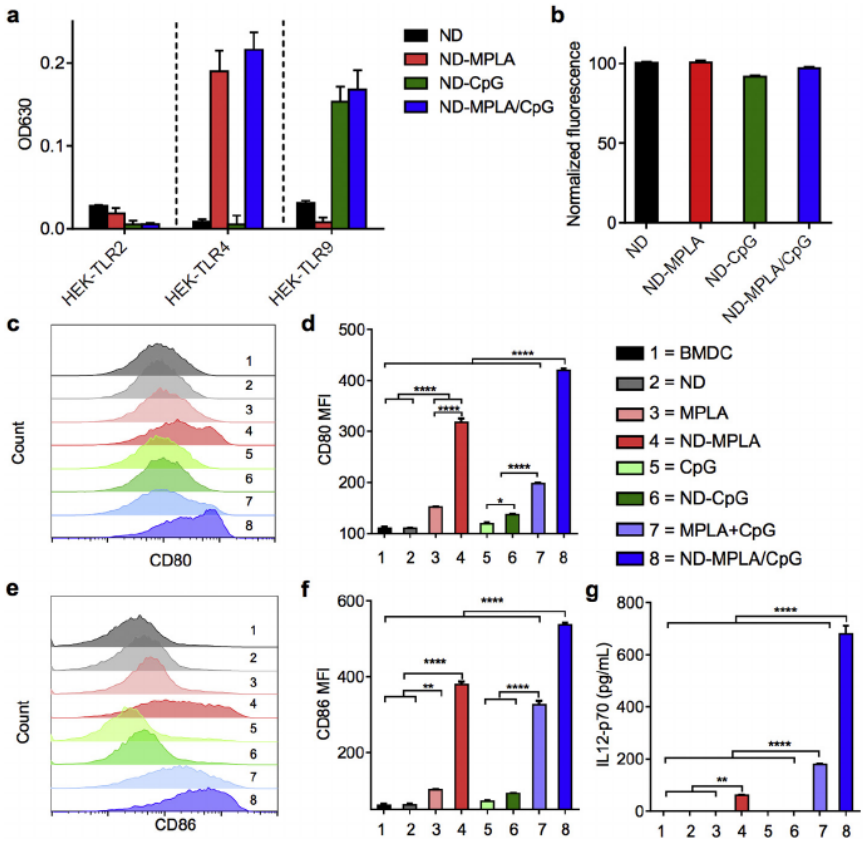

Fig. 2. Immune activation with adjuvant-loaded nanodiscs. (a) HEK-TLR2, HEK-TLR4, or HEK-TLR9 cell lines were incubated for 24 h with the indicated formulations containing 0.5 μg/mL CpG and/or 0.05 μg/mL MPLA, and activation of TLR2, TLR4, and TLR9 was measured. BMDCs were incubated for 24 h with the indicated formulations containing 0.5 μg/mL CpG and/or 0.05 μg/mL MPLA. Shown are (b) cellular uptake of DiD-labeled NDs, (c-f) activation markers, CD80 and CD86, measured by flow cytometry after staining with fluorophore-labeled antibodies. (g) The levels of IL-12p70 secreted by BMDCs incubated with various adjuvant formulations were quantified. Data show mean ± SEM from a representative experiment ($n = 3$) from 2 independent studies. $^{**}P < 0.01$, $^{****}P < 0.0001$ analyzed by one-way ANOVA with Tukey's multiple comparisons post-test.

signals on antigen-presenting cells and promote secretion of pro-inflammatory cytokines, which are required for potent elicitation of adaptive immune responses. Using HEK-TLR4 and HEK-TLR9 cell lines, we confirmed that the extent of TLR4 or TLR9 activation was similar between ND-MPLA/CpG and respective treatment with either ND-MPLA or ND-CpG (Fig. 2a), whereas TLR2 activation was minimal. These results indicated that the dual ND-MPLA/CpG adjuvant system maintained the TLR4 and TLR9 activating-capacity of MPLA and CpG. To examine the impact of ND-mediated adjuvant delivery on APCs, we incubated BMDCs in vitro with various adjuvant formulations and

evaluated costimulatory signals and cytokine release. The extent of BMDC uptake for blank ND, ND-MPLA, NP-CpG, and ND-MPLA/CpG was similar (Fig. 2b). BMDCs incubated with blank ND without any adjuvants did not upregulate co-stimulatory markers, CD80 or CD86 (Fig. 2c,d). Compared with soluble MPLA, delivery of MPLA via ND (ND-MPLA) resulted in 2-fold and 3.7-fold increases in the expression levels of CD80 and CD86, respectively ($P < 0.0001$, Fig. 2c-f). Compared with soluble CpG, delivery of CpG via ND (ND-CpG) resulted in 1.2-fold increase in the expression level of CD80 ($P < 0.05$, Fig. 2c,d). Co-delivery of MPLA and CpG in ND (ND-MPLA/CpG) led to significantly improved up-regulation of CD80 and 86, with 2.1-fold and 1.6-fold respective enhancements, compared with free admixture of MPLA and CpG ($P < 0.0001$, Fig. 2c-f). Notably, ND-MPLA/CpG improved CD80 activation by 1.3-fold and 3-fold, compared with ND-MPLA and ND-CpG, respectively ($P < 0.0001$, Fig. 2c,d). Similarly, the expression levels of CD86 were increased 1.4-fold and 5.8-fold with ND-MPLA/CpG, compared with ND-MPLA and ND-CpG, respectively ($P < 0.0001$, Fig. 2e,f). We also observed robust secretion of IL-12p70 from BMDCs treated with ND-MPLA/CpG ($P < 0.0001$, Fig. 2g), whereas other adjuvant formulations produced low or non-detectable levels of IL-12p70. Taken all together, these results indicate that ND serves as a non-immunogenic, "blank" platform upon which adjuvant(s) can be efficiently incorporated. We have also demonstrated that ND co-loaded with MPLA and CpG is more effective at activating DCs in vitro, compared with free adjuvants or even ND containing a single adjuvant.

3.3. Humoral immune responses elicited by adjuvant-loaded nanodiscs

Having shown immune activation in vitro (Fig. 2), we next sought to determine the optimal dose of ND for immunogenicity studies in vivo. Naïve C57BL/6 mice were vaccinated three times in a 2-week interval with various doses of ND-MPLA/CpG admixed with a fixed dose of 10 μg OVA protein employed as a model antigen. On day 7 after the third vaccination, we examined anti-OVA IgG titers in animal sera. The ND dose containing 1 μg MPLA and 10 μg CpG (shown as "1×" dose) was required to induce statistically significant anti-OVA IgG responses ($P < 0.05$, compared with the non-treated control, Fig. 3a). While increasing the dose of adjuvants to 2 μg MPLA and 20 μg CpG (shown as "2×" dose) improved anti-OVA IgG titers, this increase was not significantly different from the "1×" dose of OVA + ND-MPLA/CpG (Fig. 3a), perhaps due to "saturation" of the humoral immune responses at the "1×" dose. Hence, we performed the next studies using the "1×" dose of adjuvants and directly compared ND versus soluble formulations (Fig. 3b). C57BL/6 mice immunized three times with OVA + ND-MPLA/CpG ("1×" dose in each vaccine) generated strong antibody responses, achieving 13-fold and 4-fold higher anti-OVA IgG titers than OVA + ND-MPLA ($P < 0.05$) and OVA + ND-CpG (not statistically significant), respectively (Fig. 3b). A similar trend was observed when the adjuvants were administered in a free form; admixture of OVA with free MPLA and CpG (OVA + MPLA/CpG, "1×" dose) generated 13-fold and 3-fold higher anti-OVA IgG titers than OVA + MPLA ($P < 0.05$) and OVA + CpG (not statistically significant), respectively (Fig. 3b). We did not observe any statistically significant differences between anti-OVA IgG titers induced by OVA + ND-MPLA/CpG or the soluble formulation (Fig. 3b). This might be because the mixture of MPLA/CpG is already a potent adjuvant system that can achieve "saturated" humoral immune responses [20].

To validate these results in a second mouse strain with an antigen other than OVA, we performed immunization studies in Balb/c mice using ND-MPLA/CpG admixed with recombinant human PCSK9 protein. PCSK9 is known to bind to LDL receptors (LDLR) and promote degradation of LDLR responsible for recycling of cholesterol, thus inducing higher cholesterol levels [41]. Hence, blocking circulating PCSK9 with anti-PCSK9 antibodies or other therapeutics may reduce cholesterol levels, as reported in recent studies [39,42,43]. In our studies, Balb/c mice vaccinated on weeks 0, 1, and 2 with PCSK9 + ND-MPLA/CpG generated similar levels of anti-mouse PCSK9 IgG responses as the free dual adjuvants (Fig. 3c), analogous to the case with OVA protein (Fig. 3b) Interestingly, compared with the non-treated control group, animals vaccinated with ND-MPLA/CpG exhibited 17–30% reduction in their total cholesterol levels for at least 7 weeks ($P < 0.001$, Fig. 3d); however, by week 11, the total cholesterol levels returned to the normal levels ($P > 0.05$, Fig. 3d). On the other hand, the soluble MPLA/CpG formulation induced more transient reduction in the total cholesterol levels, which returned to the normal levels by week 7 ($P > 0.05$, Fig. 3d). These transient effects of anti-PCSK9 vaccines have been reported previously [42], and potentially could be overcome by reactivation of anti-PCSK9 IgG responses with boost immunizations for long-term cholesterol management [42].

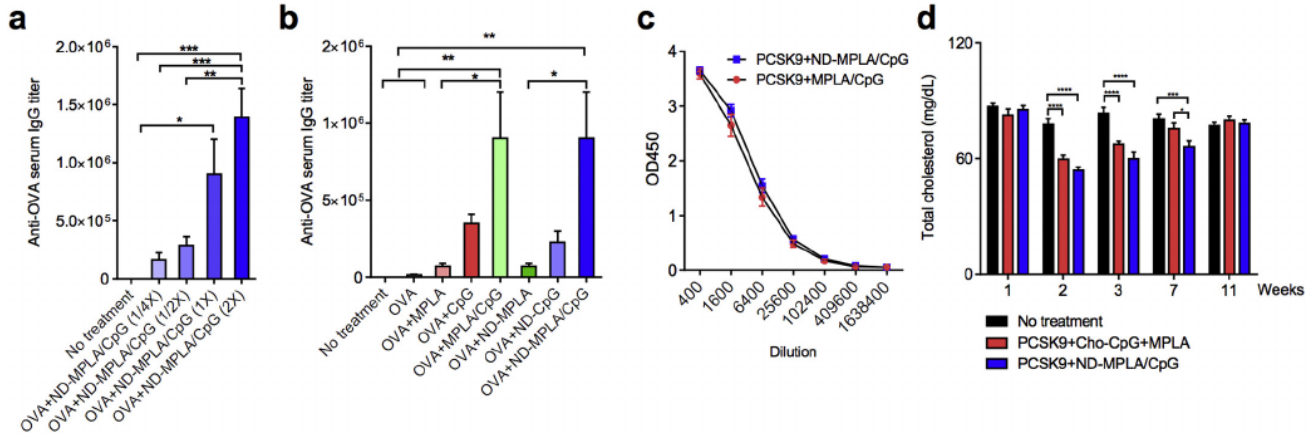

Fig. 3. Antibody responses induced by adjuvant-loaded nanodiscs. (a–b) C57BL/6 mice were vaccinated three times in a 2-week interval with 10 μg/dose of OVA admixed with the indicated adjuvants (1× = 1 μg/dose of MPLA and/or 10 μg/dose of CpG). Shown are (a) the dose dependence of the anti-OVA IgG titers and (b) the anti-OVA IgG titers induced by the indicated formulations on day 35. (c–d) Balb/c mice were vaccinated three times on weeks 0, 1, and 2 with 0.5–4 μg/dose (0.5 μg/dose for primary vaccination and 4 μg/dose for 2 booster vaccinations) of hPCSK9 admixed with the indicated adjuvants (1 μg/dose of MPLA and 10 μg/dose of CpG). Shown are (c) anti-PCSK9 IgG titers 1 week after the last vaccination and (d) the total cholesterol levels over time. Data show mean ± SEM from a representative experiment ($n = 5$) from 2 independent studies. *$P < 0.05$, **$P < 0.01$, ***$P < 0.001$ analyzed by one-way ANOVA (a–b) or two-way ANOVA (c–d) with Tukey's multiple comparisons post-test.

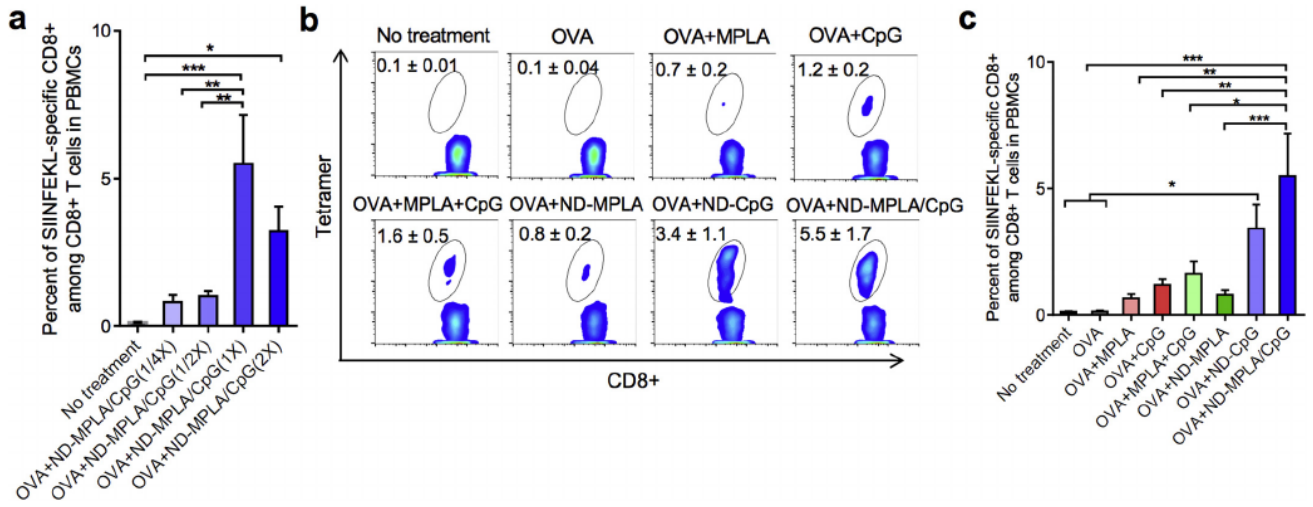

Fig. 4. Potent CD8+ T cell responses elicited by nanodiscs carrying MPLA and CpG. (a-c) C57BL/6 mice were vaccinated three times in a 2-week interval with 10 μg/dose of OVA admixed with the indicated adjuvants, and antigen-specific CD8+ T cell responses among PBMCs were quantified by the tetramer staining performed on day 35. Shown are (a) the dose dependence of antigen-specific CD8+ T cell responses with various dose of ND-MPLA/CpG, (b) the representative scatter plots, and (c) percentages of antigen-specific CD8+ T cells induced by the indicated adjuvants (1× = 1 μg/dose of MPLA and/or 10 μg/dose of CpG). Data show mean ± SEM from a representative experiment (n = 5–8) from 2 independent studies. *P < 0.05, **P < 0.01, ***P < 0.001 analyzed by one-way ANOVA with Tukey's multiple comparisons post-test.

3.4. Robust CD8+ T cell responses elicited by dual adjuvant-loaded nanodiscs

We next examined CD8+ cytotoxic T lymphocyte (CTL) responses generated by adjuvant-loaded ND. First, we determined the dose-dependence of CTL responses on ND-MPLA/CpG vaccination. Naïve C57BL/6 mice were vaccinated three times in a 2-week interval with various doses of ND-MPLA/CpG admixed with a fixed dose of 10 μg OVA protein. On day 7 after the third vaccination, we quantified the frequency of OVA-specific CD8+ T cells among peripheral blood mononuclear cells (PBMCs) by the tetramer staining assay. Vaccination with the ND dose of 1 μg MPLA and 10 μg CpG (shown as "1×" dose) elicited the highest level of SIINFEKL-tetramer+ CD8+ T cell responses at 5.5 ± 1.7% (Fig. 4a). When the dose of adjuvant was lower than 10 μg/dose CpG and 1 μg/dose MPLA, the CD8+ T cell responses were not statistically different from the non-treated control group. On the other hand, when the dose was higher than 10 μg/dose CpG and 1 μg/dose MPLA, the T cell responses started to decrease (Fig. 4a), potentially due to overt immune activation [44]. Having shown the ND co-loaded with 1 μg MPLA and 10 μg CpG as the ideal dose for T cell responses, we investigated the impact of adjuvant delivery via either ND or soluble forms on elicitation of antigen-specific CD8+ T cell responses. Three immunizations with OVA+ND-MPLA/CpG ("1×" dose) generated robust antigen-specific CD8+ T cell responses among PBMCs, achieving 3.3-fold higher frequency of SIINFEKL-tetramer+ CD8+ T cells than the equivalent dose of soluble OVA+MPLA+CpG vaccine (P < 0.05, Fig. 4b,c). OVA+ND-MPLA/CpG vaccination also enhanced antigen-specific CD8+ T cell responses, compared with OVA+ND-MPLA (a 7-fold increase, P < 0.001) and OVA+ND-CpG (a 1.6-fold increase, although this was not statistically significant) (Fig. 4b,c).

3.5. Therapeutic e cacy of vaccine nanodiscs against B16F10-OVA melanoma

Having shown that ND-MPLA/CpG induces potent cellular and humoral immune responses, we next sought to examine their efficacy as a therapeutic vaccine in tumor-bearing animals (Fig. 5a). C57BL/6 mice were inoculated with B16F10-OVA melanoma cells in the s.c. flank. On day 7 when the tumors were established with the average volume of 70 mm^3, the animals were administered s.c. at tail base with 10 μg/dose of OVA protein admixed with 1 μg/dose of MPLA and/or 10 μg/dose of CpG in either soluble or ND formulations. On 13, a boost dose was given, and on day 20, the percentages of antigen-specific CD8+ T cells among PBMCs were analyzed by the tetramer staining assay (Fig. 5a). Compared with OVA admixed with free adjuvant(s), OVA+ND-MPLA/CpG significantly enhanced antigen-specific CTL responses with ~10% tetramer+ CD8+ T cells, representing 10-fold, 4.9-fold, and 8.1-fold increases than OVA+MPLA (P < 0.0001), OVA+CpG (P < 0.001), and OVA+MPLA/CpG (P < 0.0001), respectively (Fig. 5b,c). Importantly, OVA+ND-MPLA/CpG also generated 5-fold and 2-fold higher antigen-specific CD8+ T cell responses than OVA+ND-MPLA (P < 0.001) and OVA+ND-CpG (P < 0.05), respectively (Fig. 5b,c). Moreover, OVA+ND-MPLA/CpG also generated strong anti-OVA IgG responses in these tumor-bearing animals (Fig. 5d).

We also monitored tumor growth in these animals. ND-mediated delivery of MPLA or CpG as a single adjuvant improved the therapeutic efficacy of the vaccines (Fig. 5e,f); treatments with OVA+ND-MPLA or OVA+ND-CpG led to stronger suppression of tumor progression, compared with OVA+MPLA (P < 0.0001, Fig. 5e) or OVA+CpG (P < 0.05, Fig. 5f). Importantly, treatments with OVA+ND-MPLA/CpG led to potent regression of established tumors and exerted significantly enhanced anti-tumor efficacy, compared with its soluble OVA+MPLA/CpG control (P < 0.0001, Fig. 5g). Notably, compared with all the other soluble or ND formulations, ND-MPLA/CpG vaccination generated significantly stronger T cell responses (Fig. 5b-c) and mediated tumor regression (Fig. 5g), whereas treatments with ND-MPLA, ND-CpG, or soluble MPLA/CpG admixture only resulted in maintenance of tumor size (Fig. 5e-f). Overall, these results indicate that ND carrying the dual adjuvants elicited strong and balanced cellular and humoral immune responses with potent therapeutic efficacy against established tumors.

3.6. Therapeutic e cacy of vaccine nanodiscs against HPV-associated TC-1 carcinoma

Finally, to confirm our results in a second tumor model with a tumor antigen other than OVA, we have evaluated the therapeutic efficacy of

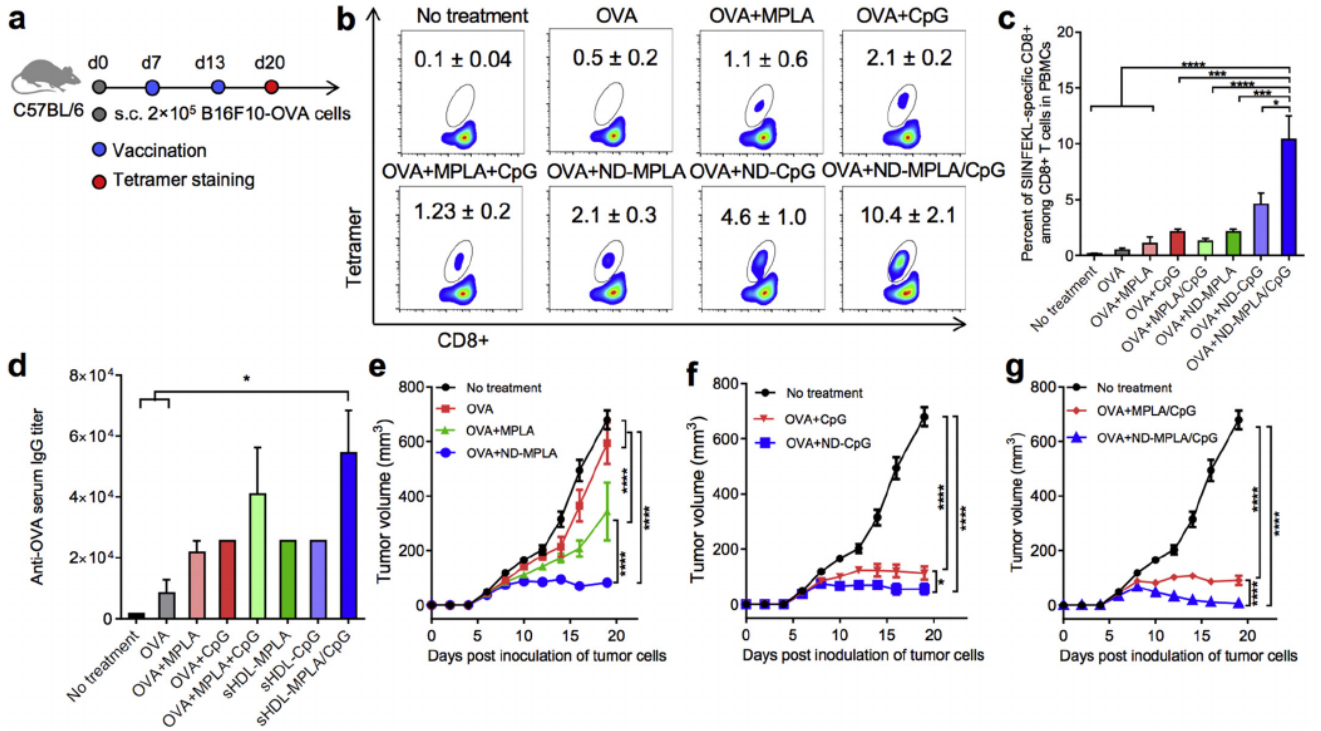

Fig. 5. Therapeutic efficacy of dual adjuvant-loaded nanodiscs against B16F10-OVA tumors. (a) C57BL/6 mice were inoculated s.c. with 2×10^5 B16F10-OVA cells on day 0. On days 7 and 13, the animals were treated with 10 μg/dose of OVA protein admixed with the indicated adjuvants (1 μg/dose of MPLA and/or 10 μg/dose of CpG). (b–c) On day 20, the percentage of OVA-specific CD8+ T cells among PBMCs were quantified by SIINFEKL-tetramer staining and flow cytometric analyses. Shown are (b) the representative scatter plots and (c) the average percentages of SIINFEKL-tetramer+ CD8+ T cells. (d) The anti-OVA IgG responses in immune sera were measured by ELISA on day 20. (e–g) The size of B16F10-OVA tumors was monitored over time. Data show mean ± SEM from a representative experiment ($n = 5$) from 2 independent studies. *$P < 0.05$, ***$P < 0.001$, ****$P < 0.0001$ analyzed by one-way ANOVA (c, d) or two-way ANOVA (e-g) with Tukey's multiple comparisons post-test.

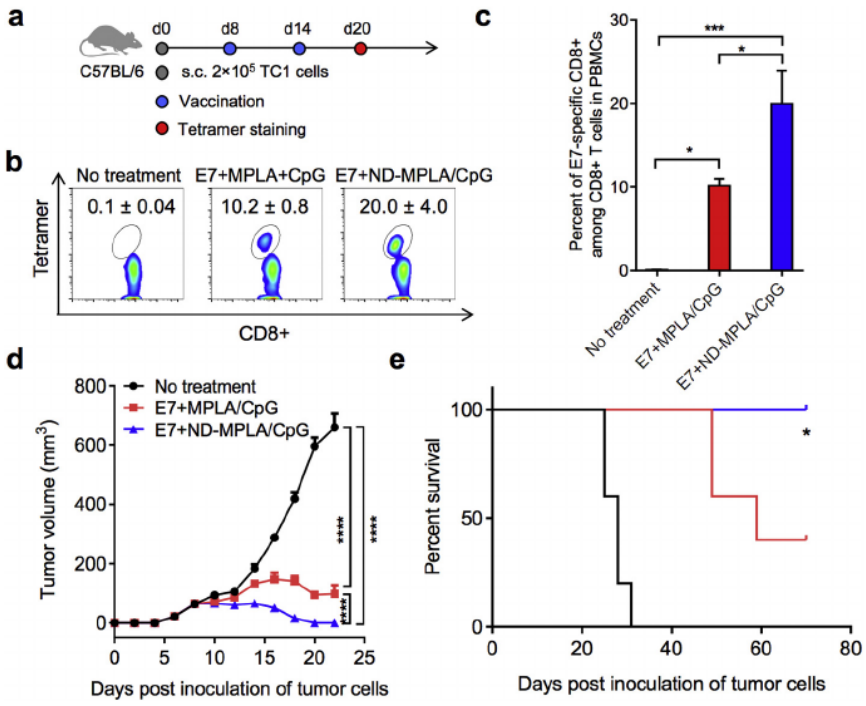

Fig. 6. Therapeutic efficacy of dual adjuvant-loaded nanodiscs against TC-1 tumors. (a) C57BL/6 mice were s.c. injected with 2×10^5 TC-1 cells on day 0. On days 8 and 14, animals were treated with 10 μg/dose of E7 peptide and indicated adjuvants containing 10 μg/dose of CpG and 1 μg/dose of MPLA. (b–c) On day 20, the percentage of E7-specific CD8+ T cells among PBMCs were quantified by tetramer staining and flow cytometric analysis. Shown are (b) the representative scatter plots and (c) the average percentages of E7-tetramer+ CD8+ T cells. Shown are (d) the size of TC-1 tumors and (e) animal survival. The asterisk in (e) indicates a statistically significant difference between E7 + MPLA/CpG and E7 + ND-MPLA/CpG. Data show mean ± SEM from a representative experiment ($n = 5$) from 2 independent studies. *$P < 0.05$, ***$P < 0.001$, ****$P < 0.0001$ analyzed by one-way ANOVA (c) or two-way ANOVA (d) with Tukey's multiple comparisons post-test, or (e) log-rank (Mantel-Cox) test.

our strategy against TC-1 cell line, which contains the E7 oncogene from human papillomavirus (HPV) type 16 [36] - a widely used preclinical model for HPV-associated cancers [45]. C57BL/6 mice were inoculated with TC-1 cells in the right flank (Fig. 6a). On day 8 when the tumors were established with the average volume of 70 mm^3, the animals were administered s.c. at tail base with 10 μg/dose of E7 peptide (GQAEPDRAHYNIVTFCCKCD, with RAHYNIVTF as the H2-D^b–restricted E7 epitope) admixed with 1 μg/dose of MPLA and/or 10 μg/dose of CpG in either soluble or ND formulations. On 14, a boost dose was given, and on day 20, the percentages of E7-specific CD8+ T cells among PBMCs were measured by the tetramer staining assay (Fig. 6a). Vaccinations with E7 + ND-MPLA/CpG markedly improved elicitation of E7-specific CD8+ T cells, achieving ~20% tetramer+ responses on day 20, which were 222-fold and 2-fold greater than those induced endogenously in non-treated, tumor-bearing mice ($P < 0.001$) and soluble E7 + MPLA/CpG treated, tumor-bearing mice ($P < 0.05$), respectively (Fig. 6b-c). Furthermore, compared with the soluble control, E7 + ND-MPLA/CpG treatment exerted significantly enhanced anti-tumor efficacy, leading to regression of TC-1 tumors ($P < 0.0001$, Fig. 6d) and all animals surviving tumor free throughout the study (Fig. 6e). Taken all together, nanodiscs co-loaded with the dual adjuvants elicit robust anti-tumor CD8+ T cell responses and inhibit established TC-1 tumors more effectively than the free dual adjuvants.

4. Conclusions

Here we report the development of homogeneous and ultrasmall nanodiscs that can co-deliver multiple adjuvants (e.g. a TLR4 agonist MPLA, and a TLR9 agonist CpG) in a synergistic manner. Nanodiscs carrying the dual adjuvants more effectively activate dendritic cells by upregulating costimulatory signals and inducing pro-inflammatory cytokines, compared with free adjuvants or nanodiscs containing a single adjuvant. Moreover, nanodiscs carrying MPLA and CpG can be simply admixed with different subunit antigens, including proteins and peptides, and elicit robust cellular and humoral immune responses in vivo. Importantly, our work demonstrates the versatility of the nanodisc system in multiple animal models. We have shown that adjuvant-loaded nanodiscs can reduce the total plasma cholesterol levels after vaccination with PCSK9 antigen and that they can exert potent anti-tumor efficacy after vaccination with tumor antigens, leading to regression of established tumors in multiple murine models. Due to its simplicity, versatility, and potency, the nanodisc system may provide a powerful delivery platform for vaccine applications against cancer, infectious diseases, and other pathologies.

Con ict of interests

A patent application for nanodisc vaccines has been filed, with J.J.M., A.S., and R.K. as inventors, and J.J.M. and A.S. are co-founders of EVOQ Therapeutics, LLC. that develops the nanodisc technology for vaccine applications.

Acknowledgements

This work was supported in part by NIH (R01EB022563, J.J.M.; R01CA210273, J.J.M.; R21NS091555, A.S.; R01HL134569, A.S.), MTRAC for Life Sciences Hub, UM Forbes Institute for Cancer Discovery Pilot Grant, and Emerald Foundation. J.J.M. is a Young Investigator supported by the Melanoma Research Alliance (348774), DoD/CDMRP Peer Reviewed Cancer Research Program (W81XWH-16-1-0369), and NSF CAREER Award (1553831). R.K. is supported by the Broomfield International Student Fellowship and the AHA Predoctoral Fellowship (15PRE25090050). W.Y. is supported by AHA Postdoctoral Fellowship (16POST27760002). L.J.O. is supported by pre-doctoral fellowships from UM Rackham and AFPE. L.S. acknowledges financial support from the UM Pharmacological Sciences Training Program (PSTP) (GM007767 from NIGMS). Opinions interpretations, conclusions, and recommendations are those of the author and are not necessarily endorsed by the Department of Defense. We acknowledge the NIH Tetramer Core Facility (contract HHSN272201300006C) for the provision of MHC-I tetramers.

References

[1] M.T. Osterholm, N.S. Kelley, A. Sommer, E.A. Belongia, Efficacy and effectiveness of influenza vaccines: a systematic review and meta-analysis, Lancet Infect. Dis. 12 (2012) 655.
[2] C.Q. Guo, M.H. Manjili, J.R. Subjeck, D. Sarkar, P.B. Fisher, X.Y. Wang, Therapeutic cancer vaccines: past, present, and future, Adv. Cancer Res. 119 (2013) 421–475.
[3] S.H. van der Burg, R. Arens, F. Ossendorp, T. van Hall, A.J.M. Melief, Vaccines for established cancer: overcoming the challenges posed by immune evasion, Nat. Rev. Cancer 16 (2016) 219–233.
[4] P.M. Moyle, I. Toth, Modern subunit vaccines: development, components, and research opportunities, ChemMedChem 8 (2013) 360–376.
[5] P. Sahdev, L.J. Ochyl, J.J. Moon, Biomaterials for nanoparticle vaccine delivery systems, Pharm. Res. 31 (2014) 2563–2582.
[6] Y.C. Fan, J.J. Moon, Nanoparticle drug delivery systems designed to improve cancer vaccines and immunotherapy, Vaccine 3 (2015) 662–685.
[7] Y.C. Fan, J.J. Moon, Particulate delivery systems for vaccination against bioterrorism agents and emerging infectious pathogens, Wiley Interdiscip. Rev. Nanomed. Nanobiotechnol. 9 (2017).
[8] J.C. Aguilar, E.G. Rodriguez, Vaccine adjuvants revisited, Vaccine 25 (2007) 3752–3762.
[9] J.K. Dowling, A. Mansell, Toll-like receptors: the swiss army knife of immunity and vaccine development, Clinical Translational Immunol. 5 (2016).
[10] T. Kawai, S. Akira, Signaling to NF-kappaB by Toll-like receptors, Trends Mol. Med. 13 (2007) 460–469.
[11] F. Steinhagen, T. Kinjo, C. Bode, D.M. Klinman, TLR-based immune adjuvants, Vaccine 29 (2011) 3341–3355.
[12] G. Napolitani, A. Rinaldi, F. Bertoni, F. Sallusto, A. Lanzavecchia, Selected Toll-like receptor agonist combinations synergistically trigger a T helper type 1-polarizing program in dendritic cells, Nat. Immunol. 6 (2005) 769–776.
[13] J.L. Garcia-Cordero, C. Nembrini, A. Stano, J.A. Hubbell, S.J. Maerkl, A high-throughput nanoimmunoassay chip applied to large-scale vaccine adjuvant screening, Integr. Biol. 5 (2013) 650–658.
[14] C.R. Casella, T.C. Mitchell, Putting endotoxin to work for us: Monophosphoryl lipid A as a safe and effective vaccine adjuvant, Cell. Mol. Life Sci. 65 (2008) 3231–3240.
[15] V. Mata-Haro, C. Cekic, M. Martin, P.M. Chilton, C.R. Casella, T.C. Mitchell, The vaccine adjuvant monophosphoryl lipid A as a TRIF-biased agonist of TLR4, Science 316 (2007) 1628–1632.
[16] H. Hacker, R.M. Vabulas, O. Takeuchi, K. Hoshino, S. Akira, H. Wagner, Immune cell activation by bacterial CpG-DNA through myeloid differentiation marker 88 and tumor necrosis factor receptor-associated factor (TRAF)6, J. Exp. Med. 192 (2000) 595–600.
[17] C. Bode, G. Zhao, F. Steinhagen, T. Kinjo, D.M. Klinman, CpG DNA as a vaccine adjuvant, Expert Rev. Vaccines 10 (2011) 499–511.
[18] A.M. Krieg, CpG motifs in bacterial DNA and their immune effects, Annu. Rev. Immunol. 20 (2002) 709–760.
[19] S. Jackson, J. Lentino, J. Kopp, L. Murray, W. Ellison, M. Rhee, G. Shockey, L. Akella, K. Erby, W.L. Heyward, R.S. Janssen, H.B.V.S. Group, Immunogenicity of a two-dose investigational hepatitis B vaccine, HBsAg-1018, using a Toll-like receptor 9 agonist adjuvant compared with a licensed hepatitis B vaccine in adults, Vaccine 36 (2018) 668–674 (PMID for Ref 19 = 29289383).
[20] V.S. Raman, A. Bhatia, A. Picone, J. Whittle, H.R. Bailor, J. O'Donnell, S. Pattabhi, J.A. Guderian, R. Mohamath, M.S. Duthie, S.G. Reed, Applying TLR synergy in immunotherapy: implications in cutaneous Leishmaniasis, J. Immunol. 185 (2010) 1701–1710.
[21] M.T. Orr, E.A. Beebe, T.E. Hudson, J.J. Moon, C.B. Fox, S.G. Reed, R.N. Coler, A dual TLR agonist adjuvant enhances the immunogenicity and protective efficacy of the tuberculosis vaccine antigen ID93, PLoS One 9 (2014) e83884.
[22] A.L. Siefert, M.J. Caplan, T.M. Fahmy, Artificial bacterial biomimetic nanoparticles synergize pathogen-associated molecular patterns for vaccine efficacy, Biomaterials 97 (2016) 85–96.
[23] R. Madan-Lala, P. Pradhan, K. Roy, Combinatorial delivery of dual and triple TLR agonists via polymeric pathogen-like particles synergistically enhances innate and adaptive immune responses, Sci. Rep. 7 (2017) 2530.
[24] T. Nakayama, J.S. Butler, A. Sehgal, M. Severgnini, T. Racie, J. Sharman, F. Ding, S.S. Morskaya, J. Brodsky, L. Tchangov, V. Kosovrasti, M. Meys, L. Nechev, G. Wang, C.G. Peng, Y.P. Fang, M. Maier, K.G. Rajeev, R. Li, J. Hettinger, S. Barros, V. Clausen, X.M. Zhang, Q.F. Wang, R. Hutabarat, N.V. Dokholyan, C. Wolfrum, M. Manoharan, V. Koteliansk, M. Stoffel, D.W.Y. Sah, Harnessing a physiologic mechanism for siRNA delivery with mimetic lipoprotein particles, Mol. Ther. 20 (2012) 1582–1589.
[25] N.O. Fischer, A. Rasley, M. Corzett, M.H. Hwang, P.D. Hoeprich, C.D. Blanchette, Colocalized delivery of adjuvant and antigen using nanolipoprotein particles enhances the immune response to recombinant antigens, J. Am. Chem. Soc. 135 (2013) 2044–2047.
[26] R. Duivenvoorden, J. Tang, D.P. Cormode, A.J. Mieszawska, D. Izquierdo-Garcia, C. Ozcan, M.J. Otten, N. Zaidi, M.E. Lobatto, S.M. van Rijs, B. Priem, E.L. Kuan,

C. Martel, B. Hewing, H. Sager, M. Nahrendorf, G.J. Randolph, E.S. Stroes, V. Fuster, E.A. Fisher, Z.A. Fayad, W.J. Mulder, A statin-loaded reconstituted high-density lipoprotein nanoparticle inhibits atherosclerotic plaque inflammation, Nat. Commun. 5 (2014) 3065.

[27] J.L. Huang, G. Jiang, Q.X. Song, X. Gu, M. Hu, X.L. Wang, H.H. Song, L.P. Chen, Y.Y. Lin, D. Jiang, J. Chen, J.F. Feng, Y.M. Qiu, J.Y. Jiang, X.G. Jiang, H.Z. Chen, X.L. Gao, Lipoprotein-biomimetic nanostructure enables efficient targeting delivery of siRNA to Ras-activated glioblastoma cells via macropinocytosis, Nat. Commun. 8 (2017).

[28] R. Kuai, D. Li, Y.E. Chen, J.J. Moon, A. Schwendeman, High-density lipoproteins: nature's multifunctional nanoparticles, ACS Nano 10 (2016) 3015–3041.

[29] C. Subramanian, R. Kuai, Q. Zhu, P. White, J.J. Moon, A. Schwendeman, M.S. Cohen, Synthetic high-density lipoprotein nanoparticles: a novel therapeutic strategy for adrenocortical carcinomas, Surgery 159 (2016) 284–294.

[30] Y. Yuan, J. Wen, J. Tang, Q.M. Kan, R. Ackermann, K. Olsen, A. Schwendeman, Synthetic high-density lipoproteins for delivery of 10-hydroxycamptothecin, Int. J. Nanomedicine 11 (2016) 6229–6238.

[31] R. Kuai, C. Subramanian, P.T. White, B.N. Timmermann, J.J. Moon, M.S. Cohen, A. Schwendeman, Synthetic high-density lipoprotein nanodisks for targeted withalongolide delivery to adrenocortical carcinoma, Int. J. Nanomedicine 12 (2017) 6581–6594.

[32] J. Tang, R. Kuai, W.M. Yuan, L. Drake, J.J. Moon, A. Schwendeman, Effect of size and pegylation of liposomes and peptide-based synthetic lipoproteins on tumor targeting, Nanomedicine-Nanotechnol. Biol. Med. 13 (2017) 1869–1878.

[33] R. Kuai, L.J. Ochyl, K.S. Bahjat, A. Schwendeman, J.J. Moon, Designer vaccine nanodiscs for personalized cancer immunotherapy, Nat. Mater. 16 (2017) 489–496.

[34] D.R. Weilhammer, C.D. Blanchette, N.O. Fischer, S. Alam, G.G. Loots, M. Corzett, C. Thomas, C. Lychak, A.D. Dunkle, J.J. Ruitenberg, S.A. Ghanekar, A.J. Sant, A. Rasley, The use of nanolipoprotein particles to enhance the immunostimulatory properties of innate immune agonists against lethal influenza challenge, Biomaterials 34 (2013) 10305–10318.

[35] M.B. Lutz, N. Kukutsch, A.L.J. Ogilvie, S. Rossner, F. Koch, N. Romani, G. Schuler, An advanced culture method for generating large quantities of highly pure dendritic cells from mouse bone marrow, J. Immunol. Methods 223 (1999) 77–92.

[36] K.Y. Lin, F.G. Guarnieri, K.F. Staveley-O'Carroll, H.I. Levitsky, J.T. August, D.M. Pardoll, T.C. Wu, Treatment of established tumors with a novel vaccine that enhances major histocompatibility class II presentation of tumor antigen, Cancer Res. 56 (1996) 21–26.

[37] M.J. Gorrin-Rivas, S. Arii, M. Furutani, M. Mizumoto, A. Mori, K. Hanaki, M. Maeda, H. Furuyama, Y. Kondo, M. Imamura, Mouse macrophage metalloelastase gene transfer into a murine melanoma suppresses primary tumor growth by halting angiogenesis, Clin. Cancer Res. 6 (2000) 1647–1654.

[38] L.J. Ochyl, J.J. Moon, Whole-animal imaging and flow cytometric techniques for analysis of antigen-specific CD8+ T cell responses after nanoparticle vaccination, J. Vis. Exp. (2015) e52771.

[39] E. Crossey, M.J.A. Amar, M. Sampson, J. Peabody, J.T. Schiller, B. Chackerian, A.T. Remaley, A cholesterol-lowering VLP vaccine that targets PCSK9, Vaccine 33 (2015) 5747–5755.

[40] J.J. Moon, H. Suh, A. Bershteyn, M.T. Stephan, H.P. Liu, B. Huang, M. Sohail, S. Luo, S.H. Um, H. Khant, J.T. Goodwin, J. Ramos, W. Chiu, D.J. Irvine, Interbilayer-crosslinked multilamellar vesicles as synthetic vaccines for potent humoral and cellular immune responses, Nat. Mater. 10 (2011) 243–251.

[41] D. Cunningham, D.E. Danley, K.F. Geoghegan, M.C. Griffor, J.L. Hawkins, T.A. Subashi, A.H. Varghese, M.J. Ammirati, J.S. Culp, L.R. Hoth, M.N. Mansour, K.M. McGrath, A.P. Seddon, S. Shenolikar, K.J. Stutzman-Engwall, L.C. Warren, D.H. Xia, X.Y. Qiu, Structural and biophysical studies of PCSK9 and its mutants linked to familial hypercholesterolemia, Nat. Struct. Mol. Biol. 14 (2007) 413–419.

[42] G. Galabova, S. Brunner, G. Winsauer, C. Juno, B. Wanko, A. Mairhofer, P. Luhrs, A. Schneeberger, A. von Bonin, F. Mattner, W. Schmidt, G. Staffler, Peptide-based anti-PCSK9 vaccines—an approach for long-term LDLc management, PLoS One 9 (2014).

[43] E.A. Stein, S. Mellis, G.D. Yancopoulos, N. Stahl, D. Logan, W.B. Smith, E. Lisbon, M. Gutierrez, C. Webb, R. Wu, Y. Du, T. Kranz, E. Gasparino, G.D. Swergold, Effect of a monoclonal antibody to PCSK9 on LDL cholesterol, N. Engl. J. Med. 366 (2012) 1108–1118.

[44] C. Volpi, F. Fallarino, M.T. Pallotta, R. Bianchi, C. Vacca, M.L. Belladonna, C. Orabona, A. De Luca, L. Boon, L. Romani, U. Grohmann, P. Puccetti, High doses of CpG oligodeoxynucleotides stimulate a tolerogenic TLR9-TRIF pathway, Nat. Commun. 4 (2013).

[45] T.H. Kang, C.P. Mao, S.Y. Lee, A. Chen, J.H. Lee, T.W. Kim, R.D. Alvarez, R.B.S. Roden, D. Pardoll, C.F. Hung, T.C. Wu, Chemotherapy acts as an adjuvant to convert the tumor microenvironment into a highly permissive state for vaccination-induced antitumor immunity, Cancer Res. 73 (2013) 2493–2504.